Z. Angew. Math. Phys. (2020) 71:8

https://doi.org/10.1007/s00033-019-1231-y

Zeitschrift für angewandte
Mathematik und Physik ZAMP

Thermocapillary migration of a planar droplet at small and large Marangoni numbers: effects of interfacial rheology

Zuo-Bing Wu

Abstract. In this paper, roles of interfacial rheology on thermocapillary migration of a planar droplet at small and large Marangoni numbers are analyzed. Under quasi-steady-state assumption, the time-independent momentum and energy equations of thermocapillary droplet migration with boundary conditions are determined. An exact solution of the steady thermocapillary migration of the deformed droplet at small Marangoni numbers is obtained. It is found that the deformed droplet has an oblate shape. The deviation from the circular section depends on the Weber number and the migration speed. The surface shear viscosity, the dilatational viscosity and the surface internal energy parameter affect the deformation of the droplet through reducing the migration speed. The validity of the steady thermocapillary droplet migration at small Marangoni numbers is confirmed by determining the conservative overall integral energy equations. At large Marangoni numbers, the non-conservative overall integral energy equations imply that thermocapillary droplet migration is always an unsteady process.

Mathematics Subject Classification. 76D45, 80A20.

Keywords. Interfacial rheology, Thermocapillary droplet migration, Quasi-steady-state assumption, Droplet deformation, Microgravity.

1. Introduction

A droplet or bubble in an external fluid can move under the influence of driving forces in the gravitational, electric and magnetic fields [1,2]. Even in the absence of body forces such as in the microgravity environment, a droplet or bubble placed in a nonisothermal matrix liquid migrates as a result of surface tension exerted on the interface. This phenomenon is termed as thermocapillary migration of the droplet or bubble. Such nonisothermal interfacial flows are very important in both the fundamental hydrodynamics and the chemical and biological engineering applications [3]. The pioneering study in this area was carried out by Young et al. (YGB) [4], who gave an analytical prediction on non-deformable droplet migration speed in the limit case of zero Reynolds(Re) and Marangoni(Ma) numbers. Then, Subramanian [5] introduced a quasi-steady-state assumption and extended the YGB results to small Re and Ma numbers. Since then, a series of results of theoretical analyses, numerical simulations and experimental investigations for thermocapillary migration of the droplet or bubble was completed [6,7].

In general, the deformation of the moving droplet or bubble depends on many factors, such as pressure, viscous stress, surface tension, interfacial rheology and so on. The most works omit an explicit consideration of the interfacial rheology on interface boundary conditions for a small surface-to-volume ratio. Taylor and Acrivos [8] and Brignell [9] determined the deformation of a falling droplet in an external fluid at small Re numbers. Bratukhin [10] and Balasubramaniam and Chai [11] obtained the solution of thermocapillary migration of a deformed droplet at small Re and Ma numbers. However, when the fluid surface-to-volume ratio increases, the interface is regarded as being material in nature. In this case, the interfacial rheology will affect the deformation of the droplet or bubble due to the force balance on the

Published online: 11 December 2019

interface [12]. Introducing the interfacial rheology, Scriven [13] derived a general formulation of the dynamics of a Newtonian fluid interface of two-phase fluids. Harper et al. [14] and Kenning [15] analyzed the effects of surface internal energy in the interfacial thermal flux balance on the motion of the droplets and bubbles in the temperature field. Levan [16] and Torres and Herbolzheimer [17] obtained the analytical solutions of thermocapillary migration of a deformed droplet and bubble with a Newton fluid interface at small Re and Ma numbers, respectively. Balasubramaniam and Subramanian [18] extended the analysis of Levan [16] for covering the inertia terms in the momentum equations and determined the deformation of a droplet under the influence of the interfacial rheology in thermocapillary migration process. Khattari et al. [19] extended the YGB solutions [4] to include effects of the interfacial rheology, the insoluble surfactant and interfacial diffusivity, and calculated the terminal migration velocity of the droplet. Manor et al. [20] found that the surface viscosity influences the droplet migration velocity quite significantly in the Marangoni migration of a droplet due to mass transfer at small Re and Peclet numbers.

The planar droplet/bubble as a simplified model was often used to study its dynamical behaviors in external liquids or on solid substrates, such as the two-dimensional(2D) bubble dynamics in a bulk liquid/a microfluid [21–24], the 2D droplet dynamics in a bulk liquid under shear stress fields [25], electric fields [26,27] and temperature fields [28,29], thermocapillary migration of a 2D droplet on solid surfaces [30–33] and thermocapillary interactions of two 2D droplets/bubbles in a bulk liquid [34,35]. On the one hand, it is assumed that the droplet/bubble is sufficiently long in the spanwise direction so that the end effects on the flow can be neglected. On the other hand, the simplified 2D droplet/bubble models can be thought as the approximate treatments of the three-dimensional droplet/bubble experiments, although their physical mechanisms may be the same or different. In this paper, we focus on roles of interfacial rheology on thermocapillary migration of a planar droplet at small and large Ma numbers in the microgravity environment. In particular, whether the interfacial rheology can change the non-conservative integral thermal flux across the surface of the droplet for preserving the overall steady-state energy balance in the flow domain in the steady thermocapillary migration at large Marangoni numbers [29] will be investigated. Section 2 describes the steady momentum and energy equations with boundary conditions under quasi-steady-state approximation. The analytical result of the steady thermocapillary migration of a deformed droplet at small Ma numbers is determined in Sect. 3. The validities of the steady thermocapillary droplet migration at small and large Ma numbers are analyzed in Sect. 4. Finally, in Sect. 5, conclusions and discussions are given.

2. Formulation under quasi-steady-state approximation

Consider the thermocapillary migration of a planar droplet in a continuous phase fluid of infinite extent under a uniform temperature gradient G. The droplet is assumed to have a slight planar deformation from the circular section with radius R_0. The temperature derivative of the interfacial tension between the droplet and the continuous phase fluid is denoted by $\sigma_T(<0)$. Two-dimensional momentum and energy equations for the continuous phase and for the fluid in the droplet in a laboratory coordinate system $(\bar{x},\bar{y})$ denoted by a bar are written as follows

$$\begin{aligned} \rho\frac{\partial\bar{\mathbf{v}}}{\partial t}+\rho\bar{\mathbf{v}}\cdot\bar{\nabla}\bar{\mathbf{v}}&=-\bar{\nabla}\bar{p}+\mu\bar{\Delta}\bar{\mathbf{v}},\\ \gamma\rho\frac{\partial\bar{\mathbf{v}}'}{\partial t}+\gamma\rho\bar{\mathbf{v}}'\bar{\nabla}\bar{\mathbf{v}}'&=-\bar{\nabla}\bar{p}'+\alpha\mu\bar{\Delta}\bar{\mathbf{v}}',\\ \frac{\partial T}{\partial t}+\bar{\mathbf{v}}\cdot\bar{\nabla}\bar{T}&=\kappa\bar{\Delta}\bar{T},\\ \frac{\partial T'}{\partial t}+\bar{\mathbf{v}}'\cdot\bar{\nabla}\bar{T}'&=\lambda\kappa\bar{\Delta}\bar{T}', \end{aligned} \tag{1}$$

where $\bar{\mathbf{v}}$, $\bar{p}$ and $\bar{T}$ are velocity, pressure and temperature, and a prime denotes quantities inside the droplet. ρ, μ and κ represent density, dynamic viscosity and thermal diffusivity of the continuous phase fluid, respectively. The correspondent values of the droplet are γ, α and λ times as large as those of the continuous phase fluid, respectively. The solutions of Eq. (1) have to satisfy boundary conditions at infinity

$$\bar{\mathbf{v}} \to 0, \quad \bar{p} \to p_\infty, \quad \bar{T} \to \bar{T}_0 + G\bar{y}, \tag{2}$$

and at the center of the droplet

$$\bar{p}' = \bar{p}'_0 + P'_0(t) \tag{3}$$

and boundary conditions at the interface $(\bar{x}_b, \bar{y}_b)$ of the two-phase fluids

$$\begin{aligned}
&\bar{\mathbf{v}}(\bar{x}_b, \bar{y}_b, t) = \bar{\mathbf{v}}'(\bar{x}_b, \bar{y}_b, t),\\
&\mathbf{n} \cdot \bar{\mathbf{\Pi}} \cdot \mathbf{n} - \mathbf{n} \cdot \bar{\mathbf{\Pi}}' \cdot \mathbf{n} = \sigma H + (\bar{\kappa}_s + \bar{\mu}_s) H (\bar{\nabla}_s \cdot \bar{\mathbf{v}}),\\
&\mathbf{n} \cdot \bar{\mathbf{\Pi}} \cdot \boldsymbol{\tau} - \mathbf{n} \cdot \bar{\mathbf{\Pi}}' \cdot \boldsymbol{\tau} = -\bar{\nabla}_s \sigma \cdot \tau - (\bar{\kappa}_s + \bar{\mu}_s) \bar{\nabla}_s (\bar{\nabla}_s \cdot \bar{\mathbf{v}}) \cdot \tau,\\
&\bar{T}(\bar{x}_b, \bar{y}_b, t) = \bar{T}'(\bar{x}_b, \bar{y}_b, t),\\
&k\frac{\partial T}{\partial n} - \beta k \frac{\partial T'}{\partial n} = (\bar{e}_s - \sigma) \bar{\nabla}_s \cdot \bar{\mathbf{v}},
\end{aligned} \tag{4}$$

where p_∞ and $\bar{T}_0$ are the undisturbed pressure and temperature of the continuous phase, respectively. $P'_0(t)$ is a function of time, which is in response to the dependence of the surface tension σ on time. $\bar{\mathbf{\Pi}}$ and $\bar{\mathbf{\Pi}}'$ are the stress tensors of the two-phase fluids. $\mathbf{n}$ and $\boldsymbol{\tau}$ are the unit vectors normal and tangent to the interface, respectively. $\bar{\nabla}_s (= \bar{\nabla} - \mathbf{n}\frac{\bar{\partial}}{\partial n})$ is the surface gradient operator. $\sigma[= \sigma_0 + \sigma_T(\bar{T} - \bar{T}_0)]$ and H are the surface tension and the curvature of the interface, respectively. $\bar{\kappa}_s$ and $\bar{\mu}_s$ denote the surface shear and dilatational viscosities, respectively. k and βk are the thermal conductivity of the continuous phase fluid and the droplet, respectively. $\bar{e}_s$ denotes the surface internal energy. It is assumed that $\bar{e}_s - \sigma (= \bar{E}_s)$ is a constant over the droplet surface.

Under the quasi-steady-state approximation, the droplet migration may achieve a quasi-steady state, i.e., migration with a constant speed V_∞. By using coordinate and variable transformations from the laboratory coordinate system to a coordinate system moving with the droplet shown schematically in Fig. 1, the momentum and energy equations (1) are derived in the Appendix and recast in dimensionless form in a polar coordinate system (r, θ) as

$$\begin{aligned}
\mathbf{v} \cdot \nabla \mathbf{v} &= -\nabla p + \frac{1}{\mathrm{Re}} \Delta \mathbf{v},\\
\gamma \mathbf{v}' \cdot \nabla \mathbf{v}' &= -\nabla p' + \frac{\alpha}{\mathrm{Re}} \Delta \mathbf{v}',\\
V_\infty + \mathbf{v} \cdot \nabla T &= \frac{1}{\mathrm{Ma}} \Delta T,\\
V_\infty + \mathbf{v}' \cdot \nabla T' &= \frac{\lambda}{\mathrm{Ma}} \Delta T'.
\end{aligned} \tag{5}$$

The coordinates, velocities and temperatures are non-dimensionalized by taking the radius of the droplet R_0, the velocity $v_0 = -\sigma_T G R_0/\mu$ and GR_0 as the reference quantities. Reynolds (Re) and Marangoni (Ma) numbers are defined as $\mathrm{Re} = \frac{\rho v_0 R_0}{\mu}$ and $\mathrm{Ma} = \frac{v_0 R_0}{\kappa}$, respectively. The boundary conditions (2)(3)(4) are rewritten in the following form of dimensionless

$$(v_r, v_\theta) \to (-V_\infty \cos\theta, V_\infty \sin\theta), \quad p \to 0, \quad T \to r\cos\theta \tag{6}$$

at infinity and

$$p' = p'_0 (= \frac{\bar{p}'_0}{\rho v_0^2}), \tag{7}$$

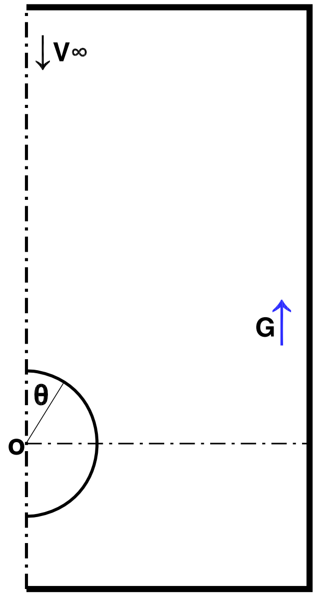

FIG. 1. A schematic diagram of thermocapillary migration of a planar droplet under the temperature gradient G in a polar coordinate system (r,θ) moving with a droplet velocity V_∞

at the center of the droplet and

$$\begin{aligned}
v_n(R,\theta) &= v'_n(R,\theta)=0,\\
v_\tau(R,\theta) &= v'_\tau(R,\theta),\\
\Pi_{nn}-\Pi'_{nn} &= \frac{\sigma^*}{We}H+\frac{\kappa_s+\mu_s}{\mathrm{Re}}H\frac{\partial v_\theta}{r\partial\theta}|_R,\\
\Pi_{n\tau}-\Pi'_{n\tau} &= \frac{1}{\mathrm{Re}}\frac{\partial T}{r\partial\theta}|_R-\frac{\kappa_s+\mu_s}{\mathrm{Re}}\frac{\partial}{r\partial\theta}(\frac{\partial v_\theta}{r\partial\theta})|_R,\\
T(R,\theta) &= T'(R,\theta),\\
\frac{\partial T}{\partial n}(R,\theta) &= \beta\frac{\partial T'}{\partial n}(R,\theta)+E_s\frac{\partial v_\theta}{r\partial\theta}|_R,
\end{aligned} \tag{8}$$

at the interface of the two-phase fluids. The interfacial rheology parameters are written in dimensionless form $\kappa_s=\bar{\kappa}_s/(\mu R_0)$, $\mu_s=\bar{\mu}_s/(\mu R_0)$ and $E_s=-\bar{E}_s\sigma_T/(\mu k)$. The Weber and Capillary numbers are defined as We=ReCa and Ca $=\frac{v_0\mu}{\sigma_0}$, respectively. The non-dimensional surface tension is reduced as $\sigma=1-\mathrm{Ca}(T+V_\infty t)=\sigma^*-\mathrm{Ca}V_\infty t$, where t is non-dimensionalized by using the reference quantity R_0/v_0. The non-dimensionalized $P'_0(t)$ in Eq. (3) is assigned as $P'_0(t)=p_\infty-\frac{1}{\mathrm{Re}}V_\infty tH\approx p_\infty-\frac{1}{\mathrm{Re}}V_\infty t$. The time-independent momentum and energy equations (5) with boundary conditions (6)–(8) reveal the steady thermocapillary droplet migration. Such the coordinate and variable transformations can thus eliminate the dependence of the solutions of steady thermocapillary migration of a deformed droplet on time [11].

3. Droplet deformation in steady thermocapillary migration at small Ma cases

The perturbated momentum and energy equations (5) of the continuous phase and the fluid in the droplet with the boundary conditions (6)–(8) for the steady thermocapillary migration of a droplet at small Re and Ma numbers are truncated at the first order and rewritten in terms of the stream functions $\Psi(r,\theta)$ and $\Psi'(r,\theta)$ as

$$\begin{aligned}\nabla^4\Psi(r,\theta)&=0,\\ \nabla^4\Psi'(r,\theta)&=0,\\ \nabla^2T(r,\theta)&=0,\\ \nabla^2T'(r,\theta)&=0\end{aligned}\tag{9}$$

and

$$\begin{aligned}&\text{(i) } \Psi(r_\infty,\theta)\to-\frac{1}{2}V_\infty r_\infty\sin\theta,\\ &\text{(ii) } \mathbf{v}'(r_0,\theta)\sim\frac{\Psi'(r,\theta)}{r}|r_0\sim O(1),\\ &\text{(iii) } v_r(1,\theta)=v'_r(1,\theta)=0,\\ &\text{(iv) } v_\theta(1,\theta)=v'_\theta(1,\theta),\\ &\text{(v) } \int_0^\pi(\Pi_{r\theta}\sin\theta-\Pi_{rr}\cos\theta)|_1\mathrm{d}\theta=0,\\ &\text{(vi) } T(1,\theta)=T'(1,\theta),\\ &\text{(vii) } \frac{\partial T}{\partial r}(1,\theta)=\beta\frac{\partial T'}{\partial r}(1,\theta)+E_s\frac{\partial v_\theta}{\partial\theta}(1,\theta),\end{aligned}\tag{10}$$

where $r_0(\to 0)$ is the center of the droplet, a small deformation of the interface is assumed as $R=1+f(\theta),|f|<<1$. Following the methods for solving the linear models [36], both the stream functions $\Psi(r,\theta)$ and $\Psi'(r,\theta)$ in Eq. (9) with the boundary conditions (i)–(iv) in Eq. (10) can be determined as

$$\begin{aligned}\Psi&=-V_\infty(r-\frac{1}{r})\sin\theta,\\ \Psi'&=-V_\infty(r^3-r)\sin\theta.\end{aligned}\tag{11}$$

The streamlines are shown in Fig. 2a. Their pattern is described as the non-separated external flow passing around the droplet and two symmetric vortices embedded in the droplet. Integrating the radial momentum equations in Eq.(5) with the boundary conditions (6), (7), both the pressure fields $p(r,\theta)$ and $p'(r,\theta)$ are given below

$$\begin{aligned}p&=V_\infty^2(\frac{1}{r^2}-\frac{1}{2r^4})\cos^2\theta-V_\infty^2(\frac{1}{r^2}+\frac{1}{2r^4})\sin^2\theta,\\ p'&=p'_0-\frac{8\alpha}{\mathrm{Re}}V_\infty r\cos\theta+\gamma V_\infty^2(r^2-\frac{1}{2}r^4)\cos^2\theta-\gamma V_\infty^2(r^2-\frac{3}{2}r^4)\sin^2\theta.\end{aligned}\tag{12}$$

In this manner, both the temperature fields $T(r,\theta)$ and $T'(r,\theta)$ in Eq. (9) with the boundary conditions (vi), (vii) in Eq. (10) are obtained as follows:

$$\begin{aligned}T&=\left(r+\frac{1-\beta-\Omega}{1+\beta+\Omega}\frac{1}{r}\right)\cos\theta,\\ T'&=\frac{2}{1+\beta+\Omega}r\cos\theta,\end{aligned}\tag{13}$$

where $\Omega=E_s/(2+2\alpha+\kappa_s+\mu_s)$. The isotherms are shown in Fig. 2b, where the curved ones appear outside the droplet, but the straight ones are inside the droplet. From the vertical force equilibrium condition (v) in Eq. (10), the steady migration velocity V_∞ is determined by inclusion of the shear stress

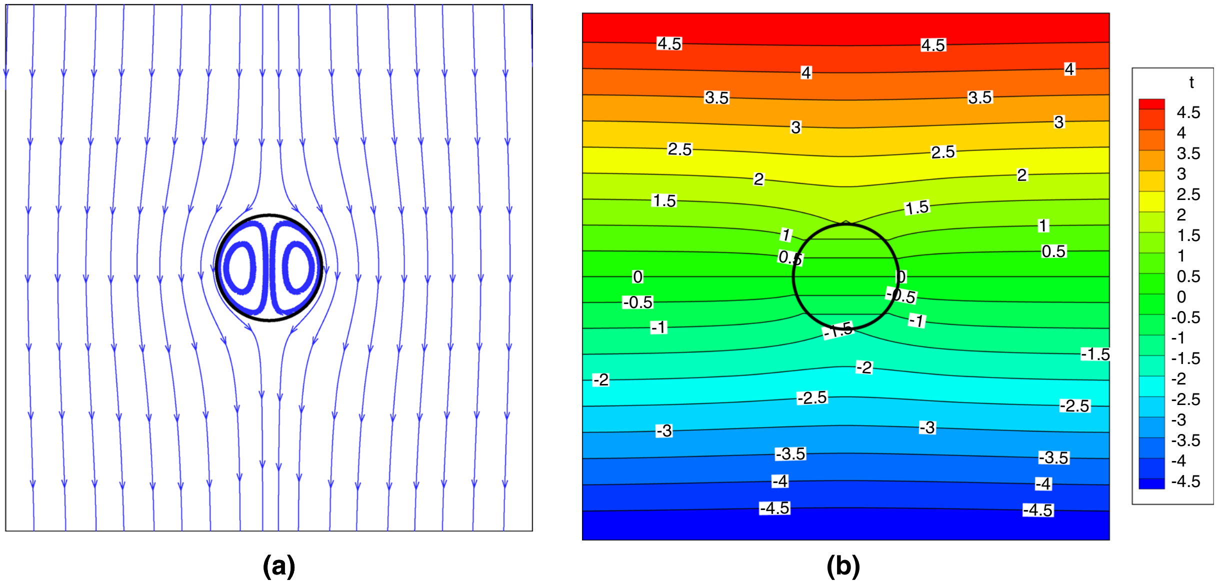

FIG. 2. **a** Streamlines and **b** isotherms in steady thermocapillary droplet migration at small Ma numbers

balance at the interface of Eq. (8) and given below

$$V_\infty = \frac{1}{(2+2\alpha+\kappa_s+\mu_s)(1+\beta+\Omega)} = \frac{\Omega}{E_s(1+\beta+\Omega)}. \tag{14}$$

It is noted that the surface shear viscosity κ_s, the dilatational viscosity μ_s and the surface internal energy parameter E_s reduce the migration speed V_∞. When κ_s, μ_s and E_s are zero, i.e., neglecting interfacial rheology, the migration speed returns to that given in [37]. Moreover, the normal stress balance at the interface of Eq. (8) can be rewritten as

$$-p + \frac{2}{\mathrm{Re}}\frac{\partial v_r}{\partial r} + p' - \frac{2\alpha}{\mathrm{Re}}\frac{\partial v_r'}{\partial r} = \frac{\sigma^*}{We}H + \frac{k_s+\mu_s}{\mathrm{Re}}H\frac{\partial v_\theta}{\partial \theta}, \tag{15}$$

where $H = (R^2+2R'^2-RR'')/(R^2+R'^2)^{3/2} \approx 1 - f(\theta) - f''(\theta)$. By substituting the solutions in Eqs. (11)(12), Eq. (15) is derived as

$$\begin{aligned} &\mathrm{Re}p_0' - \frac{\mathrm{Re}}{2}V_\infty^2(1-\gamma-4\sin^2\theta) - 4V_\infty(1+\alpha)\cos\theta \\ &\quad = \left[\frac{1}{Ca} - \frac{2}{1+\beta+\Omega}\cos\theta + 2(k_s+\mu_s)V_\infty\cos\theta\right][1-f(\theta)-f''(\theta)]. \end{aligned} \tag{16}$$

In addition to the above shear and normal stress balances at the interface, the deformed droplet in the steady thermocapillary migration is required to satisfy other conditions from the following facts. On the one hand, the area of the deformed droplet remains unchanged, which demands that

$$\int_0^\pi f(\theta)\mathrm{d}\theta = 0. \tag{17}$$

On the other hand, the center of mass of the droplet is always fixed at the origin of coordinates, which demands that

$$\int_0^\pi f(\theta)\cos\theta\mathrm{d}\theta = 0. \tag{18}$$

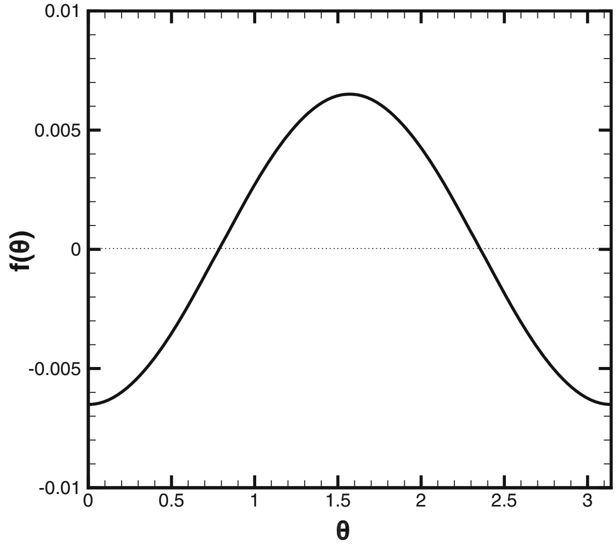

Fig. 3. Derivation $f(\theta)$ from circular section versus θ curve for steady thermocapillary migration of a planar droplet at small Ma numbers under $\alpha=\beta=\kappa_s=\mu_s=\Omega=0.2$ and $We=0.1$

By integrating Eq. (16) from 0 to π, the unknown parameter p_0' is determined as

$$\begin{aligned} p_0' &= \frac{1}{We}-\frac{1}{2}V_\infty^2(1+\gamma)-\left[\frac{1}{Ca}-\frac{2}{1+\beta+\Omega}+2(\kappa_s+\mu_s)V_\infty\right]\frac{f'(\pi)-f'(0)}{\pi Re} \\ &= \frac{1}{We}-\frac{1}{2}V_\infty^2(1+\gamma), \end{aligned} \tag{19}$$

where $f'(\pi)-f'(0)=0$ is assumed. With the parameter p_0', Eq. (16) is rewritten as

$$\begin{aligned} &\mathrm{Re}V_\infty^2\cos 2\theta+4V_\infty(1+\alpha)\cos\theta \\ &\quad = 2\left[\frac{1}{1+\beta+\Omega}-(\kappa_s+\mu_s)V_\infty\right]\cos\theta+\frac{1}{Ca}[f(\theta)+f''(\theta)]\right]. \end{aligned} \tag{20}$$

By using the expression of V_∞ in Eqs. (14), (20) can be written as

$$\mathrm{Re}V_\infty^2\cos 2\theta=\frac{1}{Ca}[f(\theta)+f''(\theta)]. \tag{21}$$

A general solution of Eq. (21) is assumed as $f(\theta)=A\cos\theta+B\cos 2\theta$, which acquires to satisfy the assumption $f'(\pi)=f'(0)$. It must have the constraints of Eqs. (17) and (18), which leads to $A=0$. Then, from Eq. (21), the unknown parameter of the solution is determined as $B=-\frac{1}{3}\mathrm{We}V_\infty^2$. Finally, the solution of Eq. (21) is written as

$$f(\theta)=-\frac{1}{3}\mathrm{We}V_\infty^2\cos 2\theta=-\frac{\mathrm{W}e}{(2+2\alpha+\kappa_s+\mu_s)^2(1+\beta+\Omega)^2}\cos 2\theta. \tag{22}$$

It is noted that the deformed droplet attains an oblate shape$[f(0)=f(\pi)<0$ and $f(\pi/2)>0]$, as shown in Fig. 3. The deformation of the droplet depends on We and V_∞. The dimensionless surface shear viscosity κ_s, the dilatational viscosity μ_s and the surface internal energy parameter E_s affect the deformation of the droplet through their influence on V_∞. When κ_s, μ_s and E_s are zero, the deformation depends on the viscosity ratio α and the conductivity ratio β of two-phase fluids, but is independent of the density ratio γ. In the case of small Ma numbers, the above assumption of the deviation $|f(\theta)|<<1$ from the circular section is thus confirmed by the fact that We and V_∞ are small.

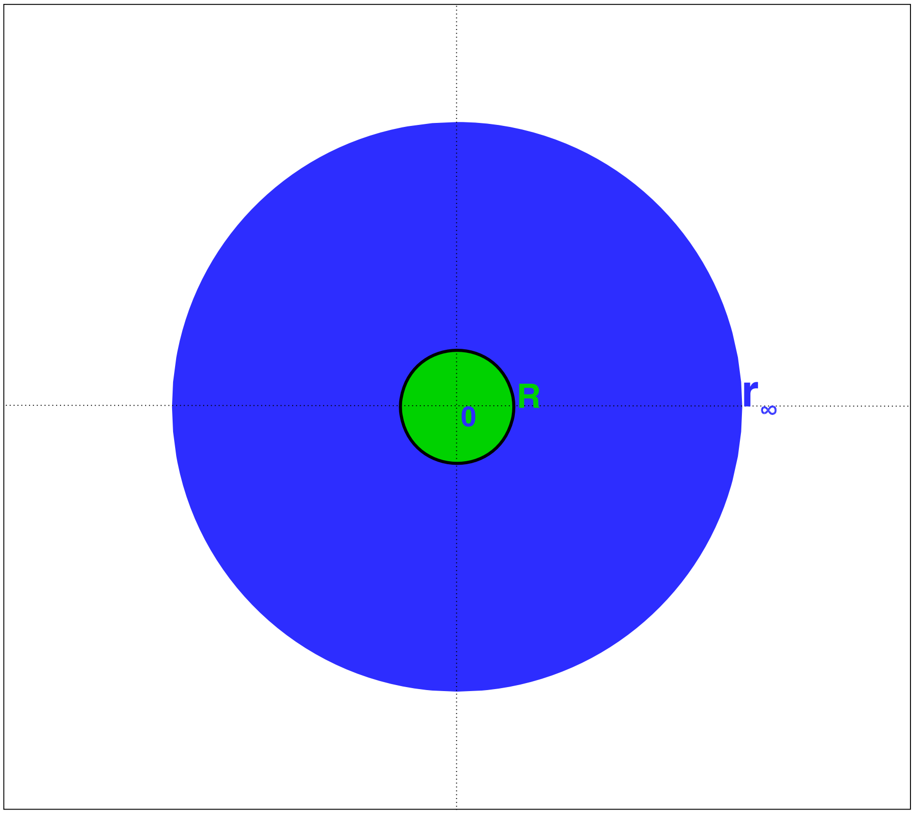

FIG. 4. The whole area of steady thermocapillary droplet migration composed of the continuous phase domain ($r \in [R, r_\infty], \theta \in [0, 2\pi]$) and the droplet region ($r \in [0, R], \theta \in [0, 2\pi]$)

4. Validities of steady thermocapillary droplet migration at small and large Ma cases

Figure 4 displays the whole area of the steady thermocapillary droplet migration composed of the continuous phase domain ($r \in [R, r_\infty], \theta \in [0, 2\pi]$) and the droplet region ($r \in [0, R], \theta \in [0, 2\pi]$). Integrating the energy equations in Eq.(5) in the continuous phase domain and the droplet region and then transforming them to linear integrals on the interface and the surface at infinite by using Green's formula, we have

$$\begin{aligned} V_\infty \left(\pi r_\infty^2 - \frac{1}{2}\int_0^{2\pi} R^2 \mathrm{d}\theta \right) + \oint (v_n T)|_{r_\infty} \mathrm{d}s = \frac{1}{Ma}\left(\oint \frac{\partial T}{\partial n}|_{r_\infty} \mathrm{d}s - \oint \frac{\partial T}{\partial n}|_R \mathrm{d}s \right), \\ \frac{V_\infty}{2}\int_0^{2\pi} R^2 \mathrm{d}\theta = \frac{\lambda}{Ma}\oint \frac{\partial T'}{\partial n}|_R \mathrm{d}s, \end{aligned} \tag{23}$$

where the normal velocity boundary condition at the interface in Eq. (8) is applied. The area of deformed droplet always keeps its original one, which may be written as

$$\frac{1}{2}\int_0^{2\pi} R^2 \mathrm{d}\theta = \pi. \tag{24}$$

Using the thermal flux boundary condition at the interface in Eq. (8), we combine Eq. (23) into the overall integral energy equation in the whole flow domain ($r \in [0, r_\infty], \theta \in [0, 2\pi]$)

$$V_\infty \pi \left(r_\infty^2 + \frac{\beta}{\lambda} - 1 \right) + \oint (v_n T)|_{r_\infty} \mathrm{d}s = \frac{1}{\mathrm{Ma}} \left[\oint \frac{\partial T}{\partial n}|_{r_\infty} \mathrm{d}s - E_s \int_0^{2\pi} \frac{\partial v_\theta}{\partial \theta}|_R \mathrm{d}\theta \right]. \quad (25)$$

It may be noticed that the non-separated velocity fields in the continuous phase fluid at infinite for large Re cases can be taken as the inviscid ones passing through a circular cylinder, which may be obtained from the lowest term of those for small Re cases in Eq.(11). We can thus assume the velocity fields

$$v_r = -V_\infty \left(1 - \frac{1}{r^2} \right) \cos\theta,$$
$$v_\theta = V_\infty \left(1 + \frac{1}{r^2} \right) \sin\theta \quad (26)$$

as those in the continuous phase fluid at infinite for any Re cases. Moreover, from Eq. (6), the temperature at infinite may be written as

$$T = T_0(r, \theta) + T_1(r, \theta) = r\cos\theta + T_1(r, \theta), \quad (27)$$

where $T_1 \to 0$ at $r \to \infty$. In final, Eq. (25) is rewritten as

$$V_\infty \pi \frac{\beta}{\lambda} + \oint (v_n T_1)|_{r_\infty} \mathrm{d}s = \frac{1}{Ma} \left[\oint \frac{\partial T_1}{\partial n}|_{r_\infty} \mathrm{d}s - E_s \int_0^{2\pi} \frac{\partial v_\theta}{\partial \theta}|_R \mathrm{d}\theta \right]. \quad (28)$$

The thermal energy $V_\infty \pi (r_\infty^2 - 1)$ of the continuous phase fluid in Eq. (25) is balanced with the convection heat transfer $\oint (v_n T_0)|_{r_\infty} ds$ in terms of T_0.

For small Ma cases, Eq. (28) is simplified as

$$\oint \frac{\partial T_1}{\partial n}|_{r_\infty} \mathrm{d}s - E_s \int_0^{2\pi} \frac{\partial v_\theta}{\partial \theta}|_R \mathrm{d}\theta = 0, \quad (29)$$

where the second term arises from energy changes during the stretching and shrinkage of interfacial area elements. The parameter $E_s << 1$ when $Re << 1$ and $\mathrm{Ma} << 1$ [14,17]. Since $T_1 \to 0$ at $r \to \infty$, the equality in Eq. (29) is confirmed, i.e., the overall integral energy equation in Eq. (25) is conservative under the quasi-steady-state assumption. It implies that thermocapillary droplet migration at small Ma cases can reach steady state. Moreover, the parameter $E_s << 1$ may approach to the above assumption of constant quantity E_s over the droplet surface. For large Ma cases, Eq. (28) is approximated as

$$V_\infty \pi \frac{\beta}{\lambda} + \oint (v_n T_1)|_{r_\infty} \mathrm{d}s + \frac{E_s}{Ma} \int_0^{2\pi} \frac{\partial v_\theta}{\partial \theta}|_R \mathrm{d}\theta = 0. \quad (30)$$

When the additional item of the temperature at infinite is taken as $T_1 = -\frac{1}{r}\cos\theta$ [29], Eq. (30) can be simplified as

$$\pi \left(\frac{\beta}{\lambda} + 1 \right) + \frac{E_s}{\mathrm{Ma}} \int_0^{2\pi} \frac{\partial (v_\theta / V_\infty)}{\partial \theta}|_R \mathrm{d}\theta = 0. \quad (31)$$

It is noticed that the first term in Eq.(31) results from contributions of the thermal energy inside the droplet and the convection heat transfer in terms of T_1. In this case, T_1 has the negative sign '$-$,' which is changed from the positive one '+' in Eq. (13) at small Ma cases for the working media in space experiments [6,7]. Meanwhile, $E_s/\mathrm{Ma} << 1$ even for a finite value $E_s[\sim O(T|_R)]$. As a result, Eq. (31) is an inequality, i.e., the overall integral energy equation in Eq. (25) is non-conservative under the quasi-steady-state assumption. Thermocapillary droplet migration at large Ma cases cannot reach any steady state and is thus an unsteady process.

5. Conclusions and discussions

In this paper, an analysis on thermocapillary migration of a planar droplet at small and large Ma numbers is performed with regard to the interfacial rheology. First, under quasi-steady-state assumption, the time-independent momentum and energy equations of steady thermocapillary droplet migration with boundary conditions are determined. Then, an exact solution of the steady thermocapillary migration of the deformed droplet at small Ma numbers is obtained. It is found that the deformed droplet has an oblate shape. The deviation from the circular section depends on the Weber number and the migration speed. The surface shear viscosity, the dilatational viscosity and the surface internal energy parameter can reduce the migration speed and affect the deformation of the droplet. Finally, validity of the steady thermocapillary droplet migration at small Ma numbers is confirmed by determining the conservative overall integral energy equations in the whole flow domain. However, at large Ma numbers, the overall integral energy equations in the whole flow domain are non-conservative, which implies the thermocapillary droplet migration is always an unsteady process.

For a single fluid in a flow domain, the conservative momentum and energy equations are always expressed in the integral forms, which include the momentum and energy transfer through all boundaries of the domain. When the flow domain as a simply-connected domain is contracted in a volume, the integral equations are valid for all choices of the volume. The differential momentum and energy equations with boundary conditions can thus be derived from the integral equations. The solutions of discretized differential equations in the domain can satisfy the integral equations. So the differential momentum and energy equations are equivalent to the integral ones [38]. For two-phase fluids with an impermeable interface in a flow domain, the conservative momentum and energy equations are still expressed in the integral forms. The flow domain as a multiply connected domain includes two subdomains for the different fluids. The differential momentum and energy equations with boundary conditions can also be derived from the integral equations. However, any given differential momentum and energy equations with boundary conditions, as the steady thermocapillary droplet migration at large Ma numbers, are not necessarily equivalent to the integral ones.

Acknowledgements

This research is supported by the National Natural Science Foundation of China through the Grants Nos. 11172310 and 11472284 and the CAS Strategic Priority Research Program XDB22040403. The author thanks the National Supercomputing Center in Tianjin for assisting in the computation.

Appendix: Steady momentum and energy equations derived from the laboratory coordinate system

Using the coordinate and variable transformations from the laboratory coordinate system $(\bar{x}, \bar{y})$ to a coordinate system (x, y) moving with the droplet velocity V_∞, respectively, described below

$$\bar{\mathbf{r}} = \mathbf{r} + V_\infty t\mathbf{j} \tag{32}$$

and

$$\begin{aligned} &\bar{\mathbf{v}}(\bar{\mathbf{r}}, t) = \mathbf{v}(\mathbf{r}) + V_\infty\mathbf{j}, \quad \bar{p}(\bar{\mathbf{r}}, t) = p(\mathbf{r}) + p_\infty, \qquad \bar{T}(\bar{\mathbf{r}}, t) - \bar{T}_0 = T(\mathbf{r}) + GV_\infty t, \\ &\bar{\mathbf{v}}'(\bar{\mathbf{r}}, t) = \mathbf{v}'(\mathbf{r}) + V_\infty\mathbf{j}, \bar{p}'(\bar{\mathbf{r}}, t) = p'(\mathbf{r}) + P_0'(t), \bar{T}'(\bar{\mathbf{r}}, t) - \bar{T}_0 = T'(\mathbf{r}) + GV_\infty t, \end{aligned} \tag{33}$$

we have

$$\begin{aligned}
\bar{\nabla}|_t &= \frac{\partial}{\partial \bar{x}}|_t\mathbf{i} + \frac{\partial}{\partial \bar{y}}|_t\mathbf{j} = \frac{\partial}{\partial x}|_t\mathbf{i} + \frac{\partial}{\partial y}|_t\mathbf{j} = \nabla|_t, \\
\bar{\Delta}|_t &= \frac{\partial^2}{\partial \bar{x}^2}|_t + \frac{\partial^2}{\partial \bar{y}^2}|_t = \frac{\partial^2}{\partial x^2}|_t + \frac{\partial^2}{\partial y^2}|_t = \Delta|_t.
\end{aligned} \tag{34}$$

For momentum equation of the continuous phase fluid in Eq. (1), we can derive its unsteady, convection and viscous terms as follows:

$$\begin{aligned}
\frac{\partial \bar{\mathbf{v}}}{\partial t}|_{\bar{\mathbf{r}}} &= \frac{\partial(\mathbf{v}+V_\infty \mathbf{j})}{\partial t}|_{\bar{\mathbf{r}}} = \frac{\partial \mathbf{v}}{\partial t}|_{\bar{\mathbf{r}}} = \frac{\partial \mathbf{v}}{\partial x}|_t \frac{\partial x}{\partial t}|_{\bar{\mathbf{r}}} + \frac{\partial \mathbf{v}}{\partial y}|_t \frac{\partial y}{\partial t}|_{\bar{\mathbf{r}}} + \frac{\partial \mathbf{v}}{\partial t}|_{\mathbf{r}} \frac{\partial t}{\partial t}|_{\bar{\mathbf{r}}} \\
&= \frac{\partial \mathbf{v}}{\partial y}|_t(-V_\infty) + \frac{\partial \mathbf{v}}{\partial t}|_{\mathbf{r}} = -V_\infty \frac{\partial \mathbf{v}}{\partial y}, \\
\bar{\mathbf{v}}\cdot\bar{\nabla}\bar{\mathbf{v}}|_t &= (\mathbf{v}+V_\infty \mathbf{j})\cdot\bar{\nabla}(\mathbf{v}+V_\infty \mathbf{j})|_t = (\mathbf{v}+V_\infty \mathbf{j})\cdot\bar{\nabla}\mathbf{v}|_{\mathbf{t}} \\
&= \mathbf{v}\cdot\nabla\mathbf{v} + V_\infty \frac{\partial \mathbf{v}}{\partial y}, \\
\bar{\nabla}\bar{p}|_t &= \bar{\nabla}(p+p_\infty)|_t = \bar{\nabla}p|_t = \nabla p, \\
\bar{\Delta}\bar{\mathbf{v}}|_t &= \bar{\Delta}(\mathbf{v}+V_\infty \mathbf{j})|_t = \bar{\Delta}\mathbf{v}|_t = \Delta\mathbf{v},
\end{aligned} \tag{35}$$

where $\frac{\partial x}{\partial t}|_{\bar{\mathbf{r}}} = \frac{\partial x}{\partial t}|_{\bar{x}} = 0$, $\frac{\partial y}{\partial t}|_{\bar{\mathbf{r}}} = \frac{\partial y}{\partial t}|_{\bar{y}} = -V_\infty$ and $\frac{\partial \mathbf{v}}{\partial t}|_{\mathbf{r}} = 0$. Then, substituting Eq. (35) into the first equation in Eq. (1), we obtain the steady momentum equation of the continuous phase fluid

$$\rho\mathbf{v}\cdot\nabla\mathbf{v} = -\nabla p + \mu\Delta\mathbf{v}. \tag{36}$$

And for energy equation of the continuous phase fluid in Eq. (1), we can write its unsteady, convection and conductivity terms as follows:

$$\begin{aligned}
\frac{\partial \bar{T}}{\partial t}|_{\bar{\mathbf{r}}} &= \frac{\partial T}{\partial t}|_{\bar{\mathbf{r}}} + GV_\infty = \frac{\partial T}{\partial x}|_t \frac{\partial x}{\partial t}|_{\bar{\mathbf{r}}} + \frac{\partial T}{\partial y}|_t \frac{\partial y}{\partial t}|_{\bar{\mathbf{r}}} + \frac{\partial T}{\partial t}|_{\mathbf{r}} \frac{\partial t}{\partial t}|_{\bar{\mathbf{r}}} + GV_\infty \\
&= \frac{\partial T}{\partial y}|_t(-V_\infty) + \frac{\partial T}{\partial t}|_{\mathbf{r}} + GV_\infty = -V_\infty \frac{\partial T}{\partial y} + GV_\infty, \\
\bar{\mathbf{v}}\cdot\bar{\nabla}\bar{T}|_t &= (\mathbf{v}+V_\infty \mathbf{j})\cdot\bar{\nabla}(T+GV_\infty t)|_t = (\mathbf{v}+V_\infty \mathbf{j})\cdot\bar{\nabla}T|_t \\
&= \mathbf{v}\cdot\nabla T + V_\infty \frac{\partial T}{\partial y}, \\
\bar{\Delta}\bar{T}|_t &= \bar{\Delta}(T+GV_\infty t)|_t = \bar{\Delta}T|_t = \Delta T,
\end{aligned} \tag{37}$$

where $\frac{\partial T}{\partial t}|_{\mathbf{r}} = 0$. Then, substituting Eq. (37) into the third equation in Eq. (1), we obtain the steady energy equation of the continuous phase fluid

$$GV_\infty + \mathbf{v}\nabla T = \kappa\Delta T. \tag{38}$$

Similarly, we can also transform the momentum and energy equations within the droplet as above.

References

[1] Sadhal, S.S., Ayyaswamy, P.S., Chung, J.N.: Transport Phenomena with Drops and Bubbles. Springer, New York (1997)
[2] Levich, V.G.: Physicochemical Hydrodynamics. Prentice-Hall International, Hemel Hempstead (1962)
[3] Subramanian, R.S., Balasubramaniam, R.: The Motion of Bubbles and Drops in Reduced Gravity. Cambridge University Press, England (2001)
[4] Young, N.O., Goldstein, J.S., Block, M.J.: The motion of bubbles in a vertical temperature gradient. J. Fluid Mech. **6**, 350 (1959)
[5] Subramanian, R.S.: Slow migration of a gas bubble in a thermal gradient. AIChE J. **27**, 646 (1981)

[6] Subramanian, R.S., Balasubramaniam, R., Wozniak, G.: Fluid mechanics of bubbles and drops. In: Monti, R. (ed.) Physics of Fluids in Microgravity. Taylor & Francis, London (2001)

[7] Yin, Z., Wu, Z.-B., Hu, W.R.: Chapter 2: Thermocapillary migration of drops and bubbles. In: Hu, W.R. (ed.) Advances in Microgravity Sciences. Transworld Research Network, Trivandrum (2009)

[8] Taylor, T.D., Acrivos, A.: On the deformation and drag of a falling viscous drop at low Reynolds number. J. Fluid Mech. **18**, 466 (1964)

[9] Beignell, A.S.: The deformation of a liquid drop at small Reynolds number. Q. J. Mech. Appl. Math. **XXVI**, 99 (1973)

[10] Bratukhin, Y.K.: Thermocapillary drift of a droplet of viscous liquid. Fluid Dyn. **10**, 833 (1975)

[11] Balasubtamaniam, R., Chai, A.-T.: Thermocapillary migration of droplet: an exact solution for small Marangoni numbers. J. Colloid Interface Sci. **119**, 531 (1987)

[12] Edwards, D.A., Brenner, H., Wasan, D.T.: Interfacial Transport Processes and Rheology. Butterworth-Heinemann, Oxford (1961)

[13] Scriven, L.E.: Dynamics of a fluid interface: equation of motion for newtonian surface fluids. Chem. Eng. Sci. **19**, 98 (1960)

[14] Happer, J.F., Moore, D.W., Pearson, J.R.A.: The effect of the variation of surface tension with temperature on the motion of bubbles and drops. J. Fluid Mech. **27**, 361 (1967)

[15] Kenning, D.B.R.: The effect of surface energy variations on the motion of bubbles and drops. Chem. Eng. Sci. **24**, 1385 (1969)

[16] Levan, M.D.: Motion of a droplet with a Newtonian interface. J. Colloid Interface Sci. **83**, 11 (1981)

[17] Torres, F.E., Herbolzheimer, E.: Temperature gradients and drag effects produced by convection of interfacial internal energy around bubbles. Phys. Fluids A **3**, 537 (1993)

[18] Balasubramaniam, R., Subramanian, R.S.: Thermocapillary migration of a drop: an exact solution with newtonian interfacial rheology and stretching/shrinkage of interfacial area elements for small Marangoni numbers. Ann. N. Y. Acad. Sci. **1027**, 303 (2004)

[19] Khattari, Z., Steffen, P., Fischer, T.M.: Migration of a droplet in a liquid: effect of insoluble surfactants and thermal gradient. J. Phys. Condens. Matter **14**, 4823 (2002)

[20] Manor, O., Lavrenteva, O., Nir, A.: Effect of non-homogeneous surface viscosity on the Marangoni migration of a droplet in viscous fluid. J. Colloid Interface Sci. **321**, 142 (2008)

[21] Delale, C.F., Tryggvason, G., Nas, S.: Cylindrical bubble dynamics: exact and direct numerical simulation results. Phys. Fluids **20**, 040903 (2008)

[22] Ilinski, Y.A., Zabolotskaya, E.A., Hay, T.A., Hamilton, M.F.: Models of cylindrical bubble pulsation. J. Acoust. Soc. Am. **132**, 1346 (2012)

[23] Wang, C., Rallabandi, B., Hilgenfeldt, S.: Frequency dependence and frequency control of microbubble streaming flows. Phys. Fluids **25**, 022002 (2013)

[24] Doinikov, A.A., Combriat, T., Thubault, P., Marmottant, P.: Acoustic streaming produced by a cylindrical bubble undergoing volume and translational oscillations in a microfluidic channel. Phys. Rev. E **94**, 033109 (2016)

[25] Zhang, J., Miksis, M.J., Bankoff, S.G.: Nonlinear dynamics of a two-dimensional viscous drop under shear flow. Phys. Fluids **18**, 072106 (2006)

[26] Mahlmann, S., Papageorgiou, D.T.: Buoyancy-driven motion of a two-dimensional bubble or drop through a viscous liquid in the presence of a vertical electric field. Theor. Comput. Fluid Dyn. **23**, 375 (2009)

[27] Zubarev, N.M., Zubareva, O.V.: Exact solutions for the shape of a 2D conducing drop moving through a dielectric medium at an angle to the external electric field. Tech. Phys. **61**, 140 (2016)

[28] Bassano, E.: Numerical simulation of thermo-solutal-capillary migration of a dissolving drop in a cavity. Int. J. Numer. Mech. Fluids **41**, 765 (2003)

[29] Wu, Z.-B., Hu, W.R.: Thermocapillary migration of a planar droplet at moderate and large Marangoni numbers. Acta Mech. **223**, 609 (2012)

[30] Smith, M.K.: Thermocapillary migration of a two-dimensional liquid droplet on a solid surface. J. Fluid Mech. **294**, 209 (1995)

[31] Savva, N., Kalliadasis, S.: Influence of gravity on the spreading of two-dimensional droplets over topographical substrates. J. Eng. Math. **73**, 3 (2012)

[32] Savva, N., Kalliadasis, S.: Low-frequency vibrations of two-dimensional droplets on heterogeneous substrates. J. Fluid Mech. **754**, 515 (2014)

[33] Sui, Y.: Moving towards the cold region or the hot region? Thermocapillary migration of a droplet attached on a horizontal substrate. Phys. Fluids **26**, 092102 (2014)

[34] Jasnow, D., Vinals, J.: Coarse-grained description of thermocapillary flow. Phys. Fluids **8**, 660 (1996)

[35] Sun, R., Hu, W.R.: Planar thermocapillary migration of two bubbles in microgravity environment. Phys. Fluids **15**, 3015 (2003)

[36] Happel, J., Brenner, H.: Low Reynolds Number Hydrodynamics. Prentice-Hall, Englewood Cliffs (1965)

[37] Wu, Z.-B.: Terminal states of thermocapillary migration of a planar droplet at moderate and large Marangoni numbers. Int. J. Heat Mass Trans. **105**, 704 (2017)
[38] Slattery, J.C.: Momentum, Energy and Mass Transfer in Continua. McGraw-Hill Book Company, New York (1972)

Zuo-Bing Wu
State Key Laboratory of Nonlinear Mechanics, Institute of Mechanics
Chinese Academy of Sciences
Beijing 100190
China
e-mail: wuzb@lnm.imech.ac.cn

Zuo-Bing Wu
School of Engineering Science
University of Chinese Academy of Sciences
Beijing 100049
China

(Received: June 16, 2019; revised: November 25, 2019)